Journal of Alloys and Compounds 382 (2004) 138–145

Journal of ALLOYS AND COMPOUNDS

www.elsevier.com/locate/jallcom

X-ray diffraction studies of thermal properties of the core and surface shell of isolated and sintered SiC nanocrystals

S. Stel'makh [a,*], S. Gierlotka [a], E. Grzanka [a,b], H.-P. Weber [c,d], B. Palosz [a]

[a] *High Pressure Research Center UNIPRESS, ul. Sokolowska 29/37, 01-142 Warsaw, Poland*
[b] *Institute of Experimental Physics, Warsaw University, ul. Hoza 69, 00-681 Warsaw, Poland*
[c] *Swiss-Norwegian Beamlines at ESRF, Grenoble, France*
[d] *Institut de Cristallographie, Université de Lausanne, CH-1015 Lausanne, Switzerland*

Received 23 October 2003; received in revised form 20 February 2004; accepted 20 February 2004

Abstract

The effect of the presence of surface strains on the apparent lattice parameters (alp) obtained experimentally for nanocrystalline SiC is discussed. The alp values were determined for two kinds of powders with an average crystallite size of 11 nm and related sintered samples. The measurements were done in a wide range of the diffractions vector up to $Q = 12\,\text{Å}^{-1}$, allowing for evaluation of the internal pressure in the grains. Based on in situ high-temperature measurements, the thermal expansion coefficient and overall temperature factor B_T were evaluated. It is shown that while the thermal expansion coefficient changes very little upon sintering, there is a large difference in the amplitude of the atomic oscillations between powders and sintered SiC reflected in a difference between respective Debye temperatures. It is concluded that the overall thermal properties of nanocrystals are determined by two components: thermal properties of the crystallite surface and its interior. The atoms at the surface vibrate much stronger than those in the bulk, and their behavior is strongly affected by the crystallite's environment.

Keywords: Nanostructures; X-ray diffraction; Thermal analysis; Synchrotron radiation

1. Introduction

Many physical properties of solids are dependent on the particle size [1–4]. The surface energy (the excess energy relative to that of the bulk material) depends on the specifications of both the bulk and the surface structures. The effect of a very small size on the atomic structure may be related to the presence of internal pressure in nanograins [5,6]. The concept of internal pressure can explain changes of the lattice parameters with the grain size. The concept can also be used to explain the presence of different phase compositions of the crystalline grains of the same material but with different grain sizes [7–10]. Internal pressure is a kind of an overall property of a given material exerted by the surface. Information about the specific atomic structure of the surface of nanocrystals would be very valuable for understanding the mechanism of generation of internal pressure. Little information on the atomic structure of the surface of nanocrystals is available in the literature, although some works show that the environment of a nanocrystal has an effect on the atomic structure of the interior of the grain [11,12]. It is also known that a change in the environment of nanocrystals can induce a phase transformation (observed, e.g., when replacing methanol with water as the pressure medium in the case of ZnS [13]). The effect of the environment is closely related to both chemical and structural changes of the crystallite surface.

The powder diffraction technique enables determination of the atomic structure of the nanocrystalline grains and allows to distinguish between the structure of the grain's interior and its surface [14,15]. However, an unambiguous determination of the structure of powders with nanometer-size grains requires the high-resolution data in a wide diffraction vector range (above 10–12 Å^{-1}). Recently, we determined the structure of the nanocrystals of SiC, diamond, and GaN with respect to the type of strains at the surface (compressive or tensile), the profile of the strain field, thickness of the surface layer, and a response of the lattice of the grain interior to the stress exerted by the surface atoms [14,15]. In the present paper, we report our first results on thermal effects in the SiC nanocrystals. The aims of our work are

* Corresponding author.
E-mail address: srvit@unipress.waw.pl (S. Stel'makh).

0925-8388/$ – see front matter © 2004 Elsevier B.V. All rights reserved.
doi:10.1016/j.jallcom.2004.05.035

determination of the thermal expansion coefficient and the overall temperature parameter B_T of the crystals. We show that the thermal properties of the nanocrystals can be properly understood only if one assumes that thermal vibrations in the grain core are different than those at its surface.

2. Experimental

2.1. Materials

Three types of SiC samples were examined: (1) two as-synthesized powders with the average grain size of 11 nm, one with the stoichiometric composition (powder I) and the other with 5% excess of carbon (powder II); (2) the same powders but sintered under high-pressure and high-temperature conditions (7.7 GPa and 1800 °C); and (3) SiC nanocomposites made with Zn and Al by a high-pressure infiltration method [16,17]. SiC powders of the average size of 11 nm were obtained from silane by laser-driven synthesis [18]. They exhibited a distribution of the grain dimensions and, therefore, their properties cannot be associated with a specific grain size. For evaluation of the grain size distribution, we used an analytical formula derived with the assumption of a log-normal grain distribution shape using peak widths measured for a single Bragg line at 1/5 and 4/5 of its maximum [19]. The distribution function shows that the dispersion of our powder is $\sigma \approx 5.5$. No grain growth was observed during fabrication of samples (II) and (III) and, therefore, we conclude that the difference between the samples is basically in the environment of the individual SiC crystallites: in a powder, each crystallite is terminated by its free surface; in SiC ceramics, the individual crystallites are in contact with other SiC crystallites; and in nanocomposites the crystallites are in contact with Zn or Al.

2.2. X-ray diffraction measurements

In-situ high-temperature X-ray powder diffraction measurements were performed at the Swiss-Norwegian Beamlines at ESRF, Grenoble in the temperature range of 130–920 K. The diffraction data were collected in the transmission geommetry using six scintillation counters and secondary beam monochromators, the wavelength of the beam was 0.05 nm. The samples were placed in the capillaries.

3. Results and discussion

3.1. Lattice parameters of nanocrystalline SiC under ambient conditions

For bulk materials, the term "lattice parameter" has a unique meaning. The situation is different in nanocrystals, which have non-uniform and complex structure. The inter-atomic distances at the surface and in the grain interior are different and, therefore, the corresponding values of the lattice parameters differ. To overcome this problem and to acquire a method for a quantitative evaluation of the diffraction data, we have recently suggested that instead of determining the poorly (for nanocrystals) defined lattice parameters one could determine quantities which we call the "apparent lattice parameters", alp values, which are associated with individual Bragg reflections [14,15]. Using the experimentally determined alp values and taking into account their characteristic dependence on the diffraction vector Q, one can evaluate the lattice parameter of the grain interior and the strains present at the crystallite surface.

The alp values measured for large diffraction vectors approach the lattice parameter of the bulk crystal. The alp values measured at low-diffraction vectors, below 4–5 $Å^{-1}$, are strongly dependent on the structure of the surface of the crystallites. The difference between the alp measured at large and small Q, $\Delta(\text{alp}/a_0)$, can be used as a measure of the difference between the corresponding inter-atomic distances in the interior and at the surface of the nanocrystals. Note that an increase of the alp at the low-Q range originates from the stresses (here: tensile) present in the surface shell. In the absence of the strains, the alp would have the similar values in the entire Q range [11,14,15].

Fig. 1 shows a dependence of the apparent lattice parameter on the diffraction vector Q (alp–Q plots) for four different nanocrystalline SiC samples: powders I and II, and sintered compacts made from these powders under 7.7 GPa at 1800 °C. We should note that to calculate alp/a_0 in Figs. 1

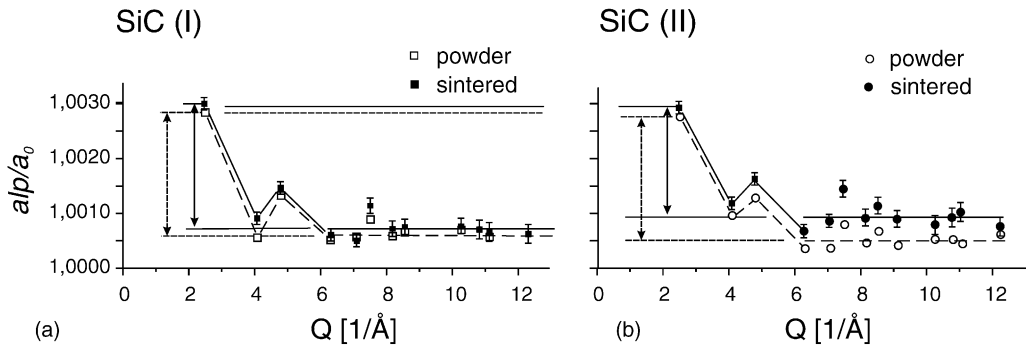

Fig. 1. Alp–Q plots of as-synthesized and sintered (7.7 GPa at 1800 °C) SiC powders: (a) pure SiC (I); and (b) SiC (II) with 5–10% carbon.

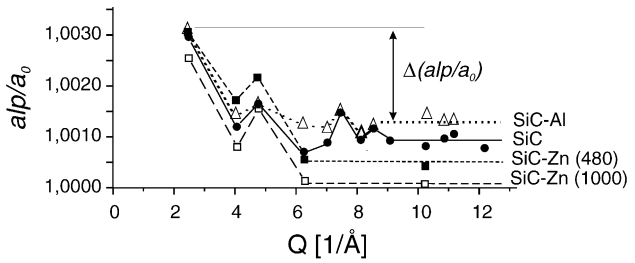

Fig. 2. Alp–Q plot of sintered nanocrystalline SiC powder II and nanocomposites made from this powder with Zn (under 8 GPa at 480 and 1000 °C) and with Al (4.5 GPa, 800 °C).

and 2, we used a_0 determined experimentally (in the same experiment) for a microcrystalline β-SiC powder. Thus, the alp/a_0 values in Figs. 1 and 2 and their deviation from unity refer to β-SiC powder used in the experiment and not to the perfect SiC crystal lattice. Consequently, the specific values of alp/a_0 cannot be used for determination of the absolute values (i.e. with respect to the perfect SiC crystal lattice) of the stresses present in the surface shell and in the grain core (internal pressure) of the examined nanocrystalline SiC samples.

To fit the line shapes, we used PeakFit 4.0 for Windows program from SPSS Science. We assumed that the difference between peak positions calculated for individual peaks using the symmetric pseudo-Voight and split Pearson shape functions is a measure of uncertainty (error bars in Fig. 1) of the experimental positions of the Bragg lines. As seen in Fig. 1, the alp values of powder I are slightly larger than those of powder II in the whole Q range. This implies that the internal pressure in sample II is slightly larger than that in sample I [5,6]. This difference can be related to an excess of carbon in sample II where carbon deposited on the surface of SiC grains generates an extra internal pressure in the grain interior. After sintering, the alp values increase for both samples, however, a much larger increase of the alp values is observed in material II. This shows that transformation of free surface of the powders into grain boundaries in the sintered materials changes the surface stresses in such a manner that the internal pressure in the grains interior is reduced; the estimated reduction in the internal pressure in sample II is about 0.4 GPa (note: the standard deviation marked with error bars in Fig. 1 is between 0.0002 and 0.0004, which corresponds to 0.1–0.3 GPa as determined from the lattice compression of SiC under hydrostatic conditions [20]). The difference in the alp values, Δ(alp/a_0), between low- and large-Q values is smaller for sintered than for powder samples (Fig. 1). The above confirms to a well-known fact that sintering is facilitated (and driven) by a reduction in interface stresses (surface energy).

Fig. 2 shows the alp–Q plot for sintered powder II and the similar plots for SiC in nanocomposites made from the same powder and Zn or Al. The content of the metals was 20 ± 2 vol.%. The pure SiC powder was sintered under 7.7 GPa at 1800 °C, the nanocomposites with Zn were obtained under 7.7 GPa at 480 and 1000 °C and those with Al under 4.5 GPa at 800 °C. There is a clear difference between the alp values determined experimentally for these samples. Because the size of the SiC crystallites is the same for all samples, the different alp values result from different environments of individual SiC nanocrystals which determine the structure of the surface and the surface stress.

In the presence of Al, the internal pressure in SiC is reduced relative to the sintered pure SiC. The difference (increase) in the alp measured for the SiC ceramics and the Al–SiC composite corresponds to compression of SiC under the pressure of about 0.3 GPa.

In the presence of Zn, the internal pressure in the SiC crystallites strongly increases. There is a difference between the SiC–Zn nanocomposites synthesized below and above the melting point (at 480 and 1000 °C, respectively). A decrease in the alp values in these composites corresponds to about 0.8 GPa in the sample made at 480 °C and to 0.4 GPa in that obtained at 1000 °C. This difference is obviously related to different surface stresses in the SiC grains (linked through the SiC–Zn grain boundaries) between samples formed at 480 and 1000 °C. The bonding between Zn and SiC is much stronger in the samples made at 1000 °C than at 480 °C, as reflected by the measured Vickers hardness of 19 and 7 GPa, respectively.

In our earlier studies, which were based on a spherical model of the SiC nanocrystals, we found that the grain core is under compressive stress while tensile stress is present in the shell. Our evaluation of the diffractograms shows, that the thickness of the surface shell in the powder is about 0.7 nm, while the surface stress is about 5–10% [15]. Apparently the change in the surrounding of the individual nanocrystals leads to a change in both the thickness of the shell and distribution of the stresses in the grain. The observed changes in the internal pressure between the sintered powders and those in the composites with Zn and Al reflect the overall effect of changes of the atomic structure and stresses at the grain surface with the environment.

3.2. Thermal expansion of nanocrystalline SiC

In general, for a crystalline material the lattice expansion can be determined from measured changes of any inter-planar spacing calculated from Bragg reflections. The problem, which we study in this work, is "the effect of the environment on the thermal properties of SiC nanocrystals". In our analysis, we refer to the model of the nanocrystal which is composed of the grain core and the surface shell and where the grain core has the perfect single crystal structure which is embedded in the surface shell. In such a case, the lattice parameter does not have a unique value and, therefore, should be replaced by the alp quantities. Therefore, we base our analysis on the alp concept, i.e. we determine the lattice expansion coefficients for specific reflections (we associate the coefficients with the corresponding diffraction vector Q) and relate the results to the

core-shell model of the nanocrystal. In view of this model, thermal expansion has two components: expansion of the grain interior and that of the surface-related structure. The alp values measured at large-Q values reflect approximately the lattice parameter of the grain interior, those measured at small Q's provide information on the properties of the grain surface. A comparison of changes of the alp observed for low- and large-Q values during heating can provide some information on difference in the thermal expansion coefficient between the grain cores and the grain surfaces. Any difference between the samples composed of the same SiC crystallites in different environments can then be interpreted as originating from different thermal properties of the surfaces of the samples.

We collected diffraction patterns of SiC samples at four different temperatures (130, 300, 640, and 920 K) and calculated the alp values for diffraction vectors of up to 12 $Å^{-1}$. The background intensity, including the diffuse scattering from the capillary was substracted from the experimental patterns. Fig. 3 shows the alp values determined experimentally for the loose and sintered powder II for three temperature intervals: 130–300 K, 300–640 K; and 640–920 K. Thermal expansion at low-temperature range is very small and falls within the accuracy of the present experiments. Thermal expansion coefficients for higher temperature intervals were calculated for three different reflections: (1 1 1), (1 1 3), and (1 1 7) ($Q = 2.4$, 4.8, and 10.3 $Å^{-1}$, respectively).

For temperature ranges 300–640 K and 640–920 K, the lattice expansion determined from the low-Q (1 1 1) reflection is slightly larger than that for large-Q reflection (1 1 7) for the powder sample. The small difference implies that the surface expands only slightly more than the core.

At the lower temperature range (300–640 K), the thermal expansion of the sintered and powder samples is the same. At higher temperatures (640–920 K), the lattice expansion coefficients calculated from the large-Q–alp values are significantly larger than that for (1 1 1) reflection for the sintered sample. This difference means that, unlike in the loose powder, the interior of SiC crystals shows larger thermal expansion than the surface.

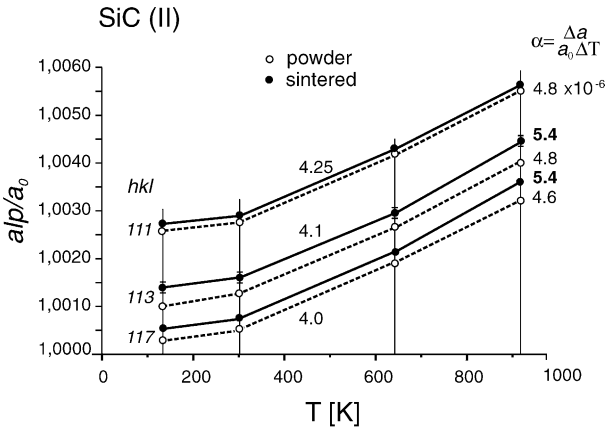

Fig. 3. Lattice expansion of powder and sintered SiC II measured for three different Bragg reflexions. Thermal expansion coefficients α are given for two temperature ranges: 300–640 K and 640–920 K. The numbers at the curves give corresponding thermal expansion coefficients in the units of 10^{-6}.

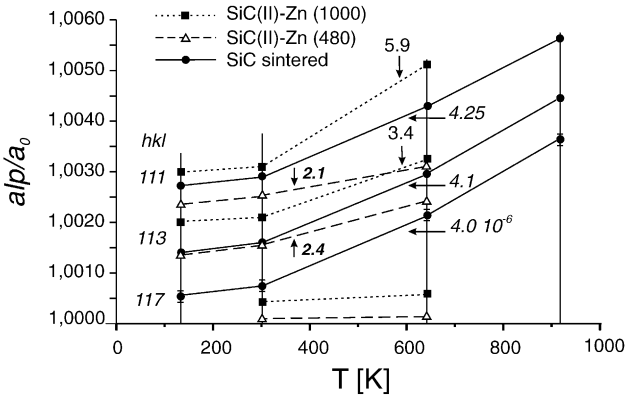

Fig. 4. Lattice expansion of sintered SiC II powder and of the same powder in a nanocomposite with Zn sintered under 8 GPa at 480 and 1000 °C.

A very strong effect of the surface on the lattice expansion in SiC grains was observed in SiC–Zn nanocomposites. In Fig. 4, we show the lattice expansion measured only up to 640 K; at higher temperatures a complex multiphase material forms, apparently as a result of inter-diffusion between Zn and SiC. SiC–Zn grain boundaries in the composites sintered at 480 and 1000 °C differ and, thus, their behavior differs as well (c.f. Fig. 2).

The thermal expansion coefficient of SiC calculated for the (1 1 1) reflection changes from 2.1×10^{-6} for the nanocomposite sample sintered at 480 °C to 5.9×10^{-6} in the sample obtained at 1000 °C. These values correspond to 50 and 150%, respectively, of the thermal expansion of pure the SiC ceramics ($\alpha = 4.25 \times 10^{-6}$).

There is no thermal expansion detected for large-Q reflection (1 1 7) for either of the composites. That means that the expansion of the interior of the grains is negligible.

The lattice expansion reflects the presence of an anharmonic component of the thermal vibrations and, thus, the extent of the expansion reflects a degree of deviation of this component from harmonicity. A very large expansion calculated from (1 1 1) reflection for SiC in Zn–SiC composite sintered at 1000 °C indicates the presence of the very strong anharmonic component of vibrations of the surface-related atoms. In the material sintered at 480 °C, this component is very small, less than that in the pure SiC sample. No changes with temperature of the alp values calculated for the (1 1 7) reflection (large Q) means that the anharmonic component of thermal vibrations in the grain interior is negligibly small.

In our experiments, we measure changes of the alp values which may be caused by different factors. One of them is an internal pressure in the grain interior (Fig. 2) which changes with an increase in temperature. The interior of SiC nanocrystals expands due to thermal vibrations. At the same time, the compressive stress from the surface (thus, compression of the grain interior) increases compensating the

vibrational expansion. As a result, the SiC–Zn composite made at 480 °C expands less than that sintered at 1000 °C when measured from the low alp values, but may show no lattice expansion at all if determined from the large *Q*–alp values because the internal pressure in the sample sintered at 1000 °C is two times larger than in that sintered at 480 °C (Fig. 2).

3.3. Thermal vibrations: overall thermal parameter B_T

It is a common practice to describe isotropic thermal vibrations using an overall temperature parameter B_T [21]. This parameter is a quantity proportional to the mean square of the atomic displacement $\langle u^2 \rangle$; $B_T = 8\,\pi^2 \langle u^2 \rangle$.

In general, one should take into account that the thermal parameter B calculated from a diffraction experiment cannot be attributed to the thermal vibrations (B_T) alone: it also includes a contribution from the static lattice distortions (B_S) existing in the individual crystalline particles ($B = B_T + B_S$). B_S may be expected to be less temperature dependent than B_T and in principle, the contribution of the static disorder B_S can be subtracted from the experimental data by analyzing its temperature dependence. This problem has been examined in detail for powders of nanocrystalline gold [22–24] where the contribution of the static disorder was evaluated from the low-temperature measurements. For our data elaboration, we assumed that the contribution from the static disorder to the experimentally determined B_T is very little, therefor we take $B = B_T$.

In a diffraction experiment, due to thermal vibrations, which increase the effective volume of the atoms, a decrease in Bragg intensities with an increase in the diffraction angle θ is observed. A change of the scattering factor for an individual atom can be described using formula (1):

$$g_j = f_{j,\theta} \exp\left[B_j \left(\frac{\sin 2\theta}{\lambda^2} \right) \right] \quad (1)$$

where $f_{j,\theta}$ is the scattering amplitude of atom j in a static lattice, and g_j is this amplitude corrected for thermal vibrations. The scattering amplitude decreases with an increase in the diffraction vector both for atomic and structural scattering amplitudes.

The B_T values can be determined experimentally from a dependence of the relative intensity of Bragg reflections on the scattering angle θ using the formula (2) given by Wilson [21–24]:

$$\log_e \left(\frac{I_{\text{exper}}}{I_{\text{calcul}}} \right) = 2 \log_e K - 2B_T \left(\frac{\sin^2 \theta_r}{\lambda^2} \right) \quad (2)$$

where K is the scaling factor associated with the structure factor $|F_o(h\,k\,l)|$:

$$I_{\text{exper}}(h\,k\,l) = K^2 |F_o(h\,k\,l)|^2 \quad (|F_o(h\,k\,l)|^2 = I_{\text{calcul}}) \quad (3)$$

According to Wilson, logarithm of the relative Bragg intensities plotted against $(\sin^2 \theta_r/\lambda^2)$ yields a straight line with the slope of $2B_T$.

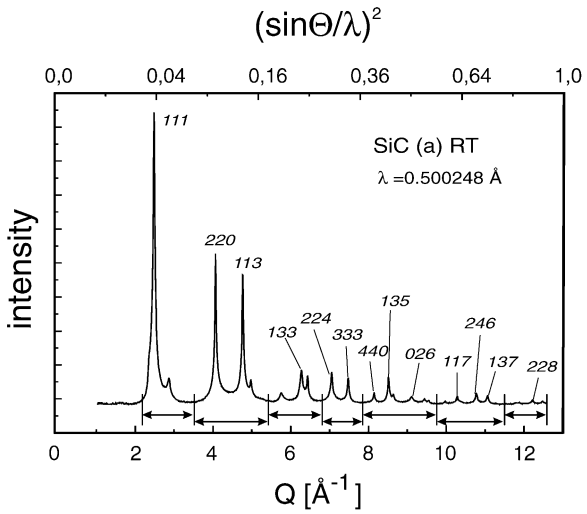

Fig. 5. Diffraction pattern of SiC II powder measured at room temperature. The double-headed arrows show angular ranges for which integral intensities were derived.

We obtained Wilson plots for SiC powders and ceramics measured at four different temperatures of 130, 300, 640, and 920 K shown in Figs. 6 and 7. The measured experimental integral intensities over selected ranges of the scattering angle $I_{\text{exper}}(\Delta 2\theta_i)$ (Fig. 5) were divided by the integral intensities calculated for the same ranges of the theoretical diffraction pattern of the cubic SiC (I_{calcul}). The theoretical patterns were calculated using DBWS-9807 Rietveld program and the Debye formula for models of spherical SiC

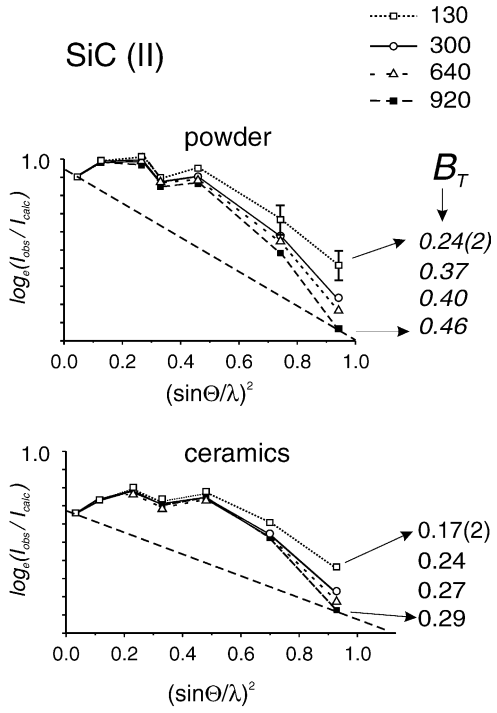

Fig. 6. Experimental Wilson plots of powder and sintered SiC II measured at four different temperatures.

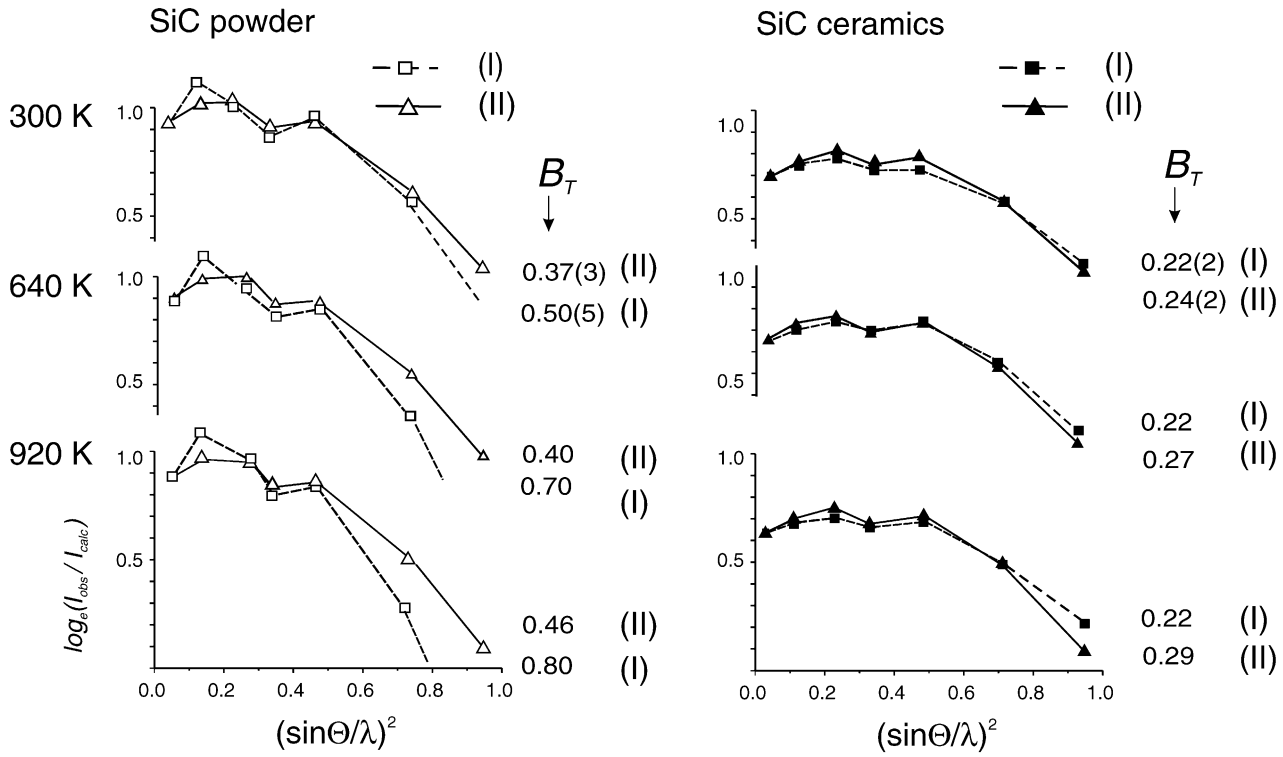

Fig. 7. Experimental Wilson plots of powders and sintered samples I and II measured at different temperatures.

nanograins with 10 nm in diameter. Both methods gave the same results.

The experimental plots in Figs. 6 and 7 exhibit a maximum in the middle part of the $(\sin\theta/\lambda)^2$ plot instead of a linear dependence of the relative intensities on $(\sin\theta/\lambda)^2$ as predicted by Wilson [21–24]. All samples show similar features. A deviation of our plots from straight line means that there is an extra intensity, additional to Bragg reflections, in the Q range of 4–10 Å^{-1}, with a maximum at about 6 Å^{-1}. This extra intensity comes probably from thermal diffuse scattering. We have to take into account also the fact that: (a) the lattice contains two kinds of atoms, Si and C which vibrate differently; and (b) that nanocrystals have a core-shell geometry and thus, two different B values are associated with such dual structure. Obviously the present data cannot be used for determination of a specific value of one, overall temperature factor B_T; we use such factor to quantify differences between samples. We made a rough evaluation of the B_T values calculated from the slope of the straight lines drawn between the first and the last point of the plots, Fig. 6. The calculated values are close to the isotropic atomic B_T values determined for bulk and single crystalline SiC crystals given in [25] ($B_{Si} = 0.2$ Å^2 and $B_C = 0.13$ Å^2).

The Wilson-type plots in Fig. 6 show that for the powders and the sintered samples the lower temperature plots are always above those obtained at higher temperatures. This reflects the fact that with an increase in temperature the thermal vibrations become more intense. The B_T values calculated from the plot increase between 130 and 920 K by a factor of nearly two. The B_T values of the powders are approximately 1.5 times larger in comparison to the sintered samples. This shows that sintering suppresses thermal vibrations in the lattice.

Fig. 7 shows Wilson-type plots of the samples fabricated from powders I and II. There is a distinct difference between the powders: the B_T values of powder I are nearly two times larger than those of powder II. This shows that in the latter, the thermal vibrations are strongly suppressed, probably by carbon deposited on the grain surfaces. While thermal vibrations are stronger in powder I, in the sintered sample I they are smaller than in the corresponding sample II.

Referring to the core-shell model of the nanocrystal, it was suggested that the temperature parameter B_T could be approximated by a sum of two corresponding components [22]:

$$B_T = pB_{core} + (1 - p)B_{shell} \quad (4)$$

Relative amount of the atoms lying on the surface (shell) related to the total number of atoms can be calculated from a simple formula: $p = 3\Delta r/r$, where r is the radius of the grain and Δr is the thickness of the surface shell. Our samples have the average grain size of 11 nm. Assuming that the thickness of the shell is 0.5 nm, the surface atoms contain 27% of all the atoms in the grain, and 55% if the shell is 1-nm thick. Thus, it is no surprise that the surface atoms have a very strong, even dominant effect on the "average thermal properties" of nanocrystals. Although using the present data, we are unable to determine the real B_T values, we are

certain that the differences between the overall B_T values of the SiC samples shown in Figs. 6 and 7 are related to the different free surface structures of the powders and to transformation of the free surfaces into the grain boundaries upon the sintering.

3.4. Evaluation of the Debye temperature

The slope of the scattering amplitude with an increase in the diffraction vector may be expected to decrease with an increase in temperature. For a bulk crystal, the temperature dependence of B_T is predicted by the Debye approximation. For very small crystallites, in which long-wavelength acoustic phonons may not exist, one can replace the Debye formula by the Einstein approximation. This is equivalent to the assumption that each atom oscillates independently with a certain frequency ν_E. In diffraction experiment, one can determine the characteristic temperature θ_E, called the Debye temperature, using the dependence of B_T on temperature (5)

$$B_T = \frac{6h^2}{mk_B\theta_E}\left\{\left[\frac{1}{\exp(\theta_E/T)} - 1\right] + \frac{1}{2}\right\} \quad (5)$$

where m, T, h and k_B are the atomic mass, the temperature, the Planck's constant and the Bolzmann constant, respectively, and θ_E is the characteristic temperature, $\theta_E = h\nu_E/k_B$.

The various values of the Debye temperature between 820 and 1430 K are given for SiC in the literature [25]. Fig. 8 shows the experimental temperature dependence of the B_T values determined for the powder and the sintered samples (Figs. 6 and 7). The figures also show the theoretical plots calculated from Eq. (5) for several temperatures using the average atomic mass of 20 (C = 12 and Si = 28). Fig. 8 shows a very large difference between the θ_E values for the powders and the sintered samples:

(i) θ_E for powder I (pure SiC) is 800 K as compared to 1000 K for powder II.
(ii) θ_E for ceramics I and II are very similar, about 1500 K, which is much larger than those for powders.

The experimental temperatures θ_E represent average values, which characterize the sample volume. For single crystals, θ_E is a property of the crystal lattice, for nanocrystals it is an overall parameter of the material, i.e. both the core and surface-shell atoms contribute to the measured θ_E. It was suggested that one can distinguish between and determine the θ_E values of the grain core and surface [23]. Our present data are only approximate and we do not attempt to calculate and interprete the specific values of B_T and θ_E. Without knowing these specific values, we can only state that the presence of the free surface atoms leads to softening of the overall thermal vibrations. The softening is very significant for powders with a large free surface area and diminishes or disappears at all after sintering, apparently due to transformation of the free surface into the grain boundaries.

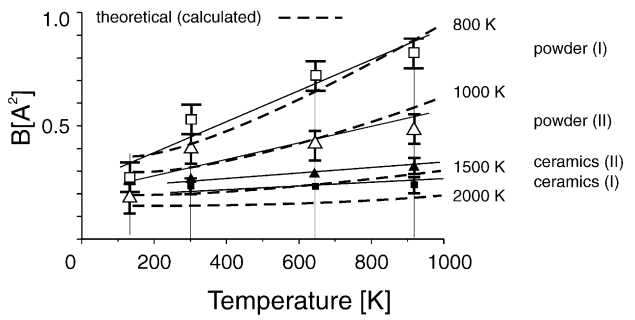

Fig. 8. Temperature dependence of the overall isotropic temperature factors B_T: experimental plots of four SiC samples and theoretical curves calculated from Eq. (5) for different characteristic temperatures θ_E.

4. Summary

Under ambient conditions, the effect of the surface is demonstrated by a difference in the lattice parameter at the surface relative to that in the interior of nanocrystals determined by the internal pressure in the grain core. We showed that thermal expansion and thermal vibrations in nanocrystalline SiC are dependent on the processing conditions of the material. The observed differences between our samples can be understood and interpreted considering that the structure of the surface is strongly influenced by the environment of the crystallites. The thermal properties of the surface have a very strong effect on the overall thermal properties of the materials. The effect of the surface on the thermal expansion of SiC is rather small for the pure powders and the sintered SiC samples. It becomes significant when the metal atoms surround the SiC crystallites. A very strong effect of the surface on the overall thermal parameter of SiC samples is also observed. The B_T values of the powders and the sintered samples are different by a factor of 2.5 at room temperature, respectively, 0.5 and 0.22 for sample I and the difference increases to a factor 4 at 920 K. Different thermal properties of the examined samples are reflected by much larger characteristic temperatures θ_E of powders than those of the sintered samples.

Acknowledgements

This work was supported by the Polish Committee for Scientific Research grant PBZ/KBN-013/T08/30, and in part by the EC Grant "Support for Centers of Excellence" no. ICA1-CT-2000-70005. The SiC powders were provided by SPAM/LFP, Laboratory "Edifices Nanometriques" from Matter Science Division, DSM, CEA, Saclay, within the Collaboration Program "Polonium", Nr 4956.I/2003. The experimental assistance from the staff of the Swiss-Norwegian Beam Lines at ESRF, Project 01-01-624, is gratefully acknowledged. The authors would like to thank Dr. Hans Boysen for valuable discussions.

References

[1] C. Suryanarayana (Ed.), Non-equilibrium Processing of Materials, Pergamon Press, Amsterdam, Lausanne, New York, Oxford, Shannon, Singapore, Tokyo, 1999.
[2] Z.L. Wang, Characterization of Nanophase Materials, Wiley-VCH, Weinheim, 2000.
[3] A. Inoue, K. Hishimoto (Eds.), Amorphous and Nanocrystalline Materials: Preparation, Properties and Applications, Springer, Berlin, 2001.
[4] J.F. Banfield, A. Navrotsky (Eds.), Nanoparticles and the Environment, Rev. Mineral. Geochem. 44, Mineralogical Society of America, 2001.
[5] R. Defay, I. Prigogine, Surface Tension and Adsorption, Longmans, Bristol, 1966.
[6] M.J. Howe (Ed.), Interfaces in Materials, Wiley, New York, 1997.
[7] J.-P. Borel, A. Chatelain, Surf. Sci. 156 (1985) 572.
[8] S.H. Tolbert, A.P. Alivisatos, J. Phys. 26 (1993) 56.
[9] S.B. Qadri, J. Yang, J.B. Ratna, E.F. Skelton, J.Z. Hu, Appl. Phys. Lett. 69 (1996) 2205.
[10] R.C. Cammarata, Mater. Sci. Eng. A 237 (1997) 180.
[11] B. Palosz, E. Grzanka, S. Gierlotka, S. Stel'makh, R. Pielaszek, U. Bismayer, J. Neuefeind, H.-P. Weber, Th. Proffen, R. Von Dreele, W. Palosz, Z. Kristallographie 217 (2002) 497.
[12] B. Palosz, E. Grzanka, S. Stel'makh, S. Gierlotka, R. Pielaszek, U. Bismayer, H.-P. Weber, Th. Proffen, W. Palosz, in: W. Lojkowski, J.R. Blizzard (Eds.), Solid State Phenomena, vol. 94, Scitec Publications, 2003, p. 203.
[13] H. Zhang, B. Gilbert, F. Huang, J.F. Banfield, Nature 424 (2003) 1025.
[14] B. Palosz, E. Grzanka, S. Gierlotka, S. Stel'makh, R. Pielaszek, W. Lojkowski, U. Bismayer, J. Neuefeind, H.-P. Weber, W. Palosz, Phase Trans. 76 (2003) 171.
[15] B. Palosz, E. Grzanka, S. Gierlotka, S. Stel'makh, R. Pielaszek, U. Bismayer, J. Neuefeind, H.-P. Weber, W. Palosz, Acta Phys. Pol., A 102 (2002) 57.
[16] E.A. Ekimov, A.G. Gavriliuk, B. Palosz, S. Gierlotka, P. Dłużewski, E. Tatianin, Yu. Kluev, A.M. Naletov, P. Biczyk, A. Grzegorczyk, A. Presz, Appl. Phys. Lett. 77 (2000) 954.
[17] S. Gierlotka, E. Grzanka, B. Palosz, M. Samulak, K. Fietkiewicz, C.H. Lathe, HASYLAB Annu. Rep., 2001.
[18] F. Huisken, B. Kohn, R. Alexandrescu, S. Cojocaru, A. Crunteanu, C. Reynaud, G. Ledoux, J. Nanopart. Res. 1 (1999) 293.
[19] R. Pielaszek, "Diffraction studies of microstructure of nanocrystals densified under high pressures", Ph.D. Thesis, Institute of Physics, Warsaw University, 2002 (in Polish).
[20] B. Palosz, S. Gierlotka, S. Stel'makh, R. Pielaszek, P. Zinn, U. Bismayer, J. Alloys Compd. 286 (1999) 184.
[21] M.F.C. Ladd, R.A. Palmer, Structure Determination by X-Ray Crystallography, Plenum Press, New York, 1994.
[22] J. Harada, S. Yao, A. Ichmiya, J. Phys. Soc. Jpn. 48 (1980) 1625.
[23] K. Oshima, A. Hatashi, J. Harada, J. Phys. Soc. Jpn. 48 (1980) 1631.
[24] J. Harada, K. Ohshima, Surf. Sci. 106 (1981) 51.
[25] A.H. Gomes de Mesquita, Acta Crystallogr. 23 (1967) 610.